

# Fabrication and Characterization of a Polymeric Microcantilever With an Encapsulated Hotwire CVD Polysilicon Piezoresistor

Nitin S. Kale, Sudip Nag, Richard Pinto, and V. Ramgopal Rao, *Senior Member, IEEE*

**Abstract**—We demonstrate a novel photoplastic nanoelectromechanical device that includes an encapsulated polysilicon piezoresistor. The temperature limitation that typically prevents deposition of polysilicon films on polymers was overcome by employing a hotwire CVD process. In this paper, we report the use of this process to fabricate and characterize a novel polymeric cantilever with an embedded piezoresistor. This device exploits the low Young's modulus of organic polymers and the high gauge factor of polysilicon. The fabricated device fits into the cantilever holder of an atomic force microscope (AFM) and can be used in conjunction with the AFM's liquid cell for detecting the adsorption of biochemicals. It enables differential measurement while preventing biochemicals from interfering with measurements using the piezoresistor. The mechanical and electromechanical characterization of the device is also reported in this paper. [2008-0108]

**Index Terms**—Affinity cantilevers, bio-microelectromechanical system (bio-MEMS), hotwire CVD (HWCVD), piezoresistive sensing, polymeric cantilevers, surface stress.

## I. INTRODUCTION

MICROCANTILEVER-BASED biosensors have attracted considerable interest to monitor a specific substance in applications such as clinical analysis, environmental control, and industrial processes [1]. The adsorption of molecules onto the surface of the cantilever generates a small-magnitude (5 to 0.5 N/m) surface stress, which results in a bending of the cantilever to the tune of a few tens of nanometers [2]–[4]. The signal detection mechanisms could be optical (deflection measurement), mass change (change in resonant frequency) [5], or even piezoresistive (strain-induced resistance change) [6], [7]. The optical readout scheme suffers from two major problems: 1) requirement to realign the laser system when liquids with different refractive indexes are used and 2) inability of making measurements with opaque liquids [3]. Laser alignment is not required for piezoresistive detection; therefore, issues with processing in opaque liquids and their refractive indexes simply disappear. As the signal from the

piezoresistive detection scheme is an electrical signal, one can build appropriate electronics around it to amplify and process the signal. However, the piezoresistive scheme is less sensitive and noisier than the optical detection scheme [3].

In this paper, for the first time, we present the fabrication and characterization of a novel polymeric cantilever that includes an embedded polysilicon piezoresistor. These cantilevers can be used for the sensing of biochemicals. The device can fit into the cantilever holder of an atomic force microscope (AFM), and therefore, it can be used in conjunction with an AFM's liquid cell for biochemical detection. Antibodies, such as antimyoglobin, can be immobilized on one surface of the cantilever inside the AFM's liquid cell. The scheme can then be used to detect myoglobin, a cardiac marker, which is released when a person has a heart attack [4].

*SU-8* is a negative tone chemically amplified near UV photoresist; it is highly resistant to chemicals, and hence, it can be used as a component material [8]. A method to modify the *SU-8* surface and make it amenable for biomolecule immobilization has been invented [9]. Fabricating a structural layer *SU-8* is a low-cost extremely low thermal budget process. *SU-8* can be spin coated and defined, and can thus provide a thin film without recourse to the conventional deposition techniques. Second, *SU-8* with its low Young's modulus (5 GPa), has a higher propensity for bending, compared to, for example, silicon nitride (150–350 GPa), for a given surface stress.

The basic design and fabrication issues in polymeric cantilevers for bio-microelectromechanical system (bio-MEMS) applications were studied using extensive simulations and reported earlier [10]. Thermal budget limitation was the critical unresolved technology issue that prevented the integration of a polysilicon film with a polymer such as *SU-8*. Low-pressure and plasma-enhanced CVD processes normally used for polysilicon deposition were ruled out for the same reason. We resolved this crucial issue by employing polysilicon, deposited by the low-temperature hotwire CVD (HWCVD) method, as the piezoresistive material. The details of the HWCVD process are out of the scope of this paper; however, a thorough treatment of the same is available in [11].

Differential measurement was identified to be another crucial issue. For example, for a single cantilever described in [12], the temperature sensitivity was estimated to be about 70 nm/°C, if a single-ended measurement was made. However, in their differential cantilever system, the differential thermal sensitivity was estimated to be only 1.4 nm/°C. Therefore, for bio-MEMS

Manuscript received April 30, 2008; revised September 8, 2008. This work was supported by the Government of India under the National Program on Smart Materials and Structures and the Nanotechnology Project. Subject Editor A. J. Ricco.

The authors are with Centre for Nanoelectronics and the Department of Electrical Engineering, Indian Institute of Technology Bombay, Mumbai 400 076, India (e-mail: nsk@ee.iitb.ac.in; sudip@ee.iitb.ac.in; rpinto@ee.iitb.ac.in; rrao@ee.iitb.ac.in).

Color versions of one or more of the figures in this paper are available online at <http://ieeexplore.ieee.org>.

Digital Object Identifier 10.1109/JMEMS.2008.2008577

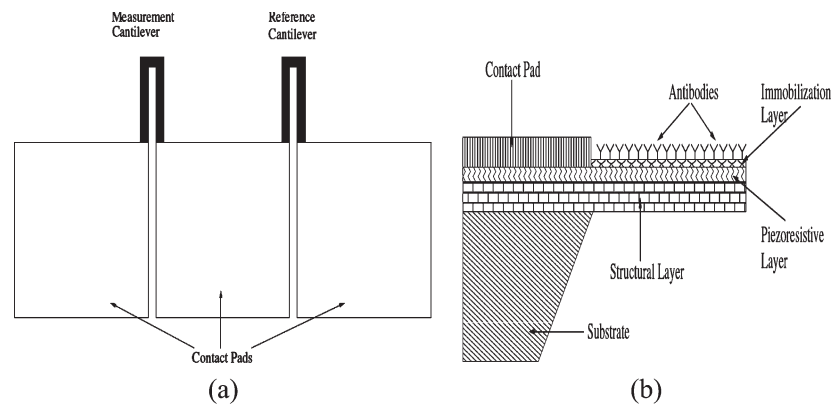


Fig. 1. Piezoresistive cantilever: (a) plan view and (b) section view.

applications, where deflections are on the order of tens of nanometers (typically up to 100 nm), it was deemed essential to employ a differential detection scheme. For a differential measurement, one cantilever acts as the measurement cantilever (i.e., on which antibodies are allowed to immobilize), while the other acts as the reference cantilever. When a measurement is made, both cantilevers experience the same environment, i.e., temperature, mechanical noise, liquid viscosity, and turbulence, thereby making differential measurement possible.

The basic piezoresistive detection scheme is shown in Fig. 1. The plan view in Fig. 1(a) shows two cantilevers connected in a half-bridge configuration. The sectional view of a piezoresistive cantilever is shown in Fig. 1(b). The bottom polymeric layer (SU-8) acts as the *structural* layer, the *middle* layer is the embedded piezoresistive layer (HWCVD polysilicon), and the top polymeric layer (SU-8) functions as a thin *immobilization* layer. Piezoresistors are therefore embedded in both cantilevers. The top polymeric layer also prevents biochemicals from interfering with the embedded piezoresistor, thereby preventing any electrical short.

## II. DESIGN ISSUES

### A. Stiffness

The stiffness or spring constant of the cantilever is an important design parameter. An affinity cantilever designed to detect biochemicals has to undergo several wet process steps such as silanization, linker attachment, and antibody immobilization. These processes involve repeated cantilever insertion into various liquids and its subsequent drying. Thus, an affinity cantilever should be stiff enough to withstand the forces involved at the air–liquid interface during the different wet processes. However, the cantilever should also be compliant enough, so that it responds to the small magnitude surface stress generated due to biomolecular recognition. Therefore, the stiffness of a cantilever is an optimization issue that should satisfy these extremes.

### B. Resonant Frequency

The resonant frequency of a microcantilever is another important design parameter. Microcantilevers could be affected by various sources of external noise. For example, the micro-

cantilever may pickup mechanical vibrations from a pump in the vicinity of the measurement setup. It was recommended in [3] that, for surface-stress-sensitive cantilevers, their resonant frequency should be higher than 5 kHz, so that they are not affected by the noise from the surroundings.

### C. Shape of SU-8/Polysilicon/SU-8 Cantilevers and the Die

The shape of the cantilevers was chosen to be of U-type to enable electromechanical characterization. The die dimensions were designed such that it could be fitted in the cantilever holder of an AFM. This enables the measurement of the resonant frequency of the cantilever for the purpose of calibration. The resonant frequency of the device can be measured by exploiting various components of the AFM setup, namely: piezo stage, laser, position sensitive detector, and feedback electronics. The piezo stage can be used to vibrate the cantilever, while the remaining components track and register the vibrations. Therefore, the die mask dimension was drawn to be  $1.6 \times 3.4$  mm.

Thus, with this test structure, one could perform the mechanical and electromechanical characterization of the polymer-piezoresistive microcantilever. Also, the same device can be used in conjunction with an AFM's liquid cell attachment to perform immobilization-related experiments.

A quick estimate of the stiffness of the cantilever was made by simulating the structure in Coventorware. However, the actual mechanical characterization of the device comprises measurement of the stiffness (by deflecting the sample cantilever with a standard cantilever) and resonant frequency of the cantilever. For electromechanical characterization, we measured the change in voltage across the piezoresistive cantilever (due to a strain-induced change in its resistance) by bending the cantilever at its tip with the help of a micromanipulator.

### D. Simulation Study

The length, width, and thickness of the cantilever are the geometric parameters that impact the stiffness of the cantilever. The Young's modulus of the materials that make the cantilever also affects its stiffness. A schematic with drawn mask dimensions of the SU-8/polysilicon/SU-8 cantilever is shown in Fig. 2(a). The SU-8/polysilicon/SU-8 cantilever was meshed using a Manhattan parabolic mesh as shown in Fig. 2(b). The detailed methodology and material properties of SU-8 and

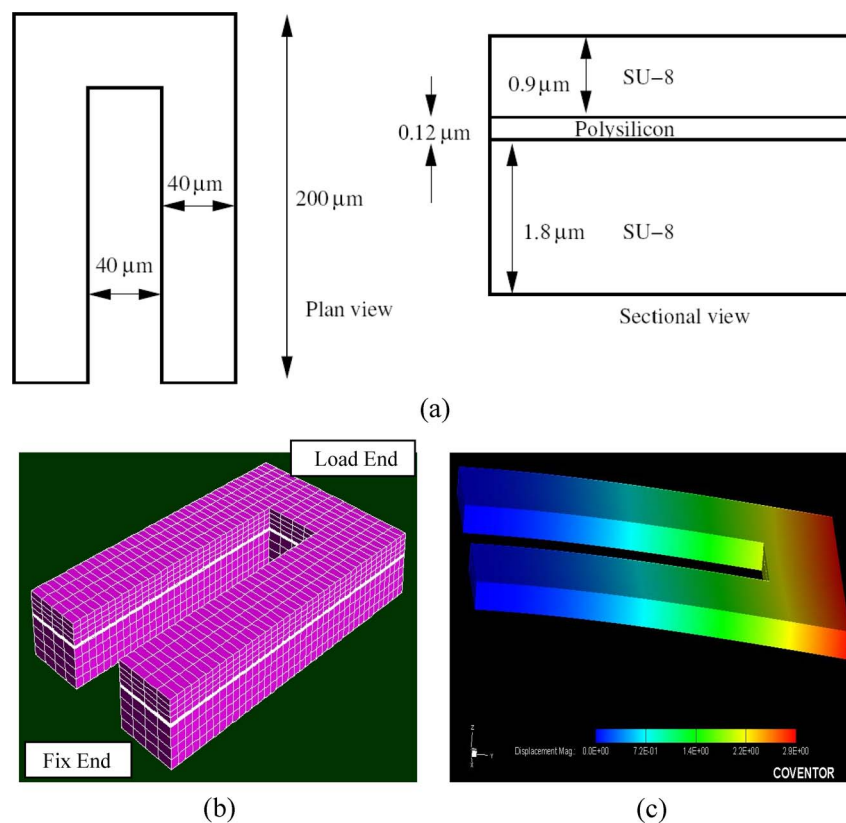


Fig. 2. (a) Planar and sectional view of a SU-8/polysilicon/SU-8 cantilever. (b) Meshed cantilever of (a). (c) Deflected cantilever of (b).

polysilicon that were employed to carry out the simulation are already reported in [10] and, hence, are not repeated in this paper. The cantilevers were simulated using the *Coventorware* simulation tool to compute their stiffness. The cantilever was fixed at its “Fix” end, and a  $1\text{-}\mu\text{N}$  force was applied at the tip of the cantilever (labeled as the “Load” end). The stiffness  $K$  is calculated as  $K = dF/dz$  where  $dF$  is the change in force applied ( $1\text{ }\mu\text{N}$ ) and  $dz$  is the deflection in the cantilever measured at its tip. The deflected SU-8 cantilever is shown in Fig. 2(c). Using the deflection data from the simulation result, we calculated the stiffness of the SU-8/polysilicon/SU-8 cantilever to be  $0.31\text{ N/m}$ . The computed value of stiffness is compared with the measured value later in this paper.

### III. DEVICE FABRICATION

#### A. SU-8/Polysilicon/SU-8 Cantilevers

To fabricate the structure, a series of deposit, pattern, and etch steps were employed. Fig. 3(a)–(h) shows the main steps of the five-mask fabrication process. First, a 2-in diameter  $\langle 100 \rangle$ -oriented silicon wafer was cleaned with piranha ( $1 : 3\text{H}_2\text{O}_2 : \text{H}_2\text{SO}_4$ ), followed by the RCA cleaning procedure. A  $\langle 100 \rangle$ -oriented wafer was chosen so that it could be diced easily for release experiments.

#### B. Selection of Sacrificial Layer

Sputter-deposited silicon dioxide was employed as a sacrificial layer primarily because it formed a uniform smooth

interface and was readily etchable in hydrofluoric acid at a high etch rate. The thickness of the sacrificial layer was  $200\text{ nm}$ .

#### C. Structural Layer

The structural layer was formed as follows. A  $1.8\text{-}\mu\text{m}$  SU-8 2002 layer was spun at  $3000\text{ r/min}$  on the substrate. It was then subjected to a soft bake at  $70\text{ }^\circ\text{C}$  for  $5\text{ min}$ , followed by UV exposure (Mask 1) for  $20\text{ s}$ . The exposed SU-8 was subjected to a postexposure bake of  $95\text{ }^\circ\text{C}$  for  $5\text{ min}$ . The substrate was then immersed in SU-8 developer for  $1\text{ min}$  and then transferred into isopropyl alcohol. This step yielded the bottom layer, i.e., structural layer of the cantilever [Fig. 3(b) and (i)].

#### D. Piezoresistive Layer

Polysilicon was deposited on the SU-8/substrate using the HWCVD process. The substrate heater temperature was maintained at  $170\text{ }^\circ\text{C}$ , the gas flow rate ratio (silane: hydrogen: diborane) of  $5 : 100 : 1$  was employed, and a process pressure of  $1.1 \times 10^{-1}\text{ mbar}$  was maintained [11]. The deposition was carried out for  $20\text{ min}$ , which yielded a polysilicon film that was  $120\text{ nm}$  thick [Fig. 3(c)]. Patterns on the polysilicon film were defined (Mask 2) using positive photoresist (*Shipley 1813*). The film was patterned by dissolving the unprotected polysilicon in HNA (hydrofluoric acid + nitric acid + deionized water). The resultant pattern yielded the piezoresistive polysilicon layer, which is shown in Fig. 3(d) and (j).

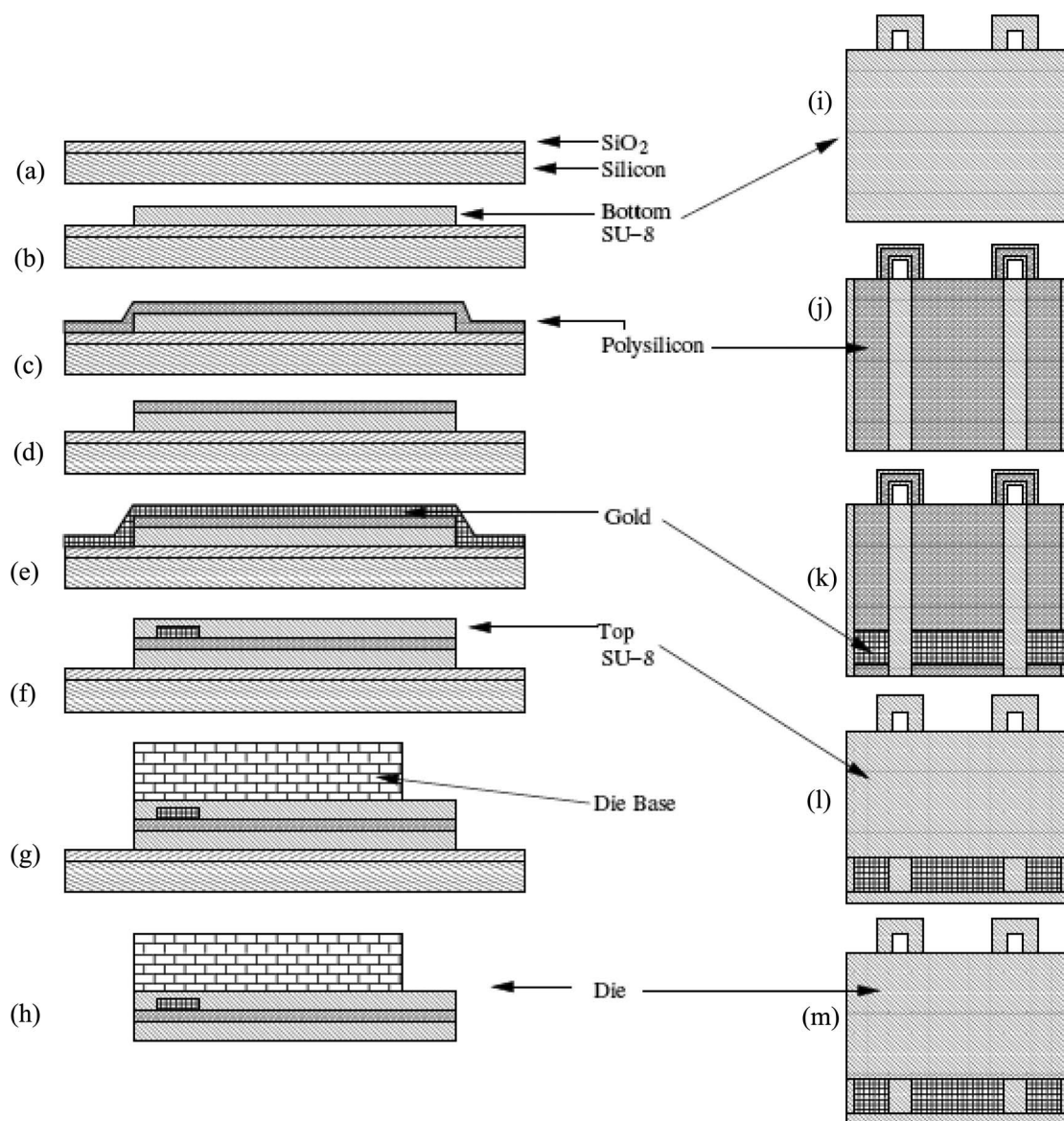


Fig. 3. (a)–(m) Process sequence to fabricate SU-8/polysilicon/SU-8 cantilevers.

### E. Contact Pads

Next, a 100-nm film of chrome–gold was deposited in a *Nordiko* sputter system on the polysilicon/SU-8/substrate. While the purpose of the gold film was to provide an electrical contact to the polysilicon layer, the intermediate chromium film improved the adhesion of the gold film with the polysilicon layer. The chrome–gold layer was defined with another level of photolithography (Mask 3). Gold was etched using a solution of potassium iodide (KI) and iodine in water, while the chromium layer was etched using a solution of ceric ammonium nitrate and acetic acid in water. Thus, the chrome–gold layer formed a contact pad to make an electrical contact with the polysilicon layer [Fig. 3(e) and (k)].

### F. Immobilization Layer

The encapsulation of the polysilicon piezoresistor was essential so that the biochemicals do not short the piezoresistors.

The top *SU-8* encapsulation layer was also the *immobilization* layer of the device. This *SU-8* layer can be subjected to HWCVD-induced dissociated ammonia treatment [9] so as to make it amenable for antibody immobilization. Therefore, another layer of *SU-8* that encapsulated the polysilicon was defined (Mask 4). Its thickness was  $0.9\ \mu\text{m}$ , which was obtained using the *SU-8 2002* diluted with its thinner in 1 : 1 proportion. The process parameters mentioned earlier for processing the bottom layer (prebake, UV exposure, postexposure bake, and development) were employed [Fig. 3(f) and (l)]. The thickness of the top *SU-8* layer was designed smaller than the bottom *SU-8* layer to keep the axis of the piezoresistive layer away from the neutral axis of the cantilever stack [10].

### G. Die Base

As mentioned earlier, the planar dimensions of the die (Mask 5) were chosen such that the device could fit into the

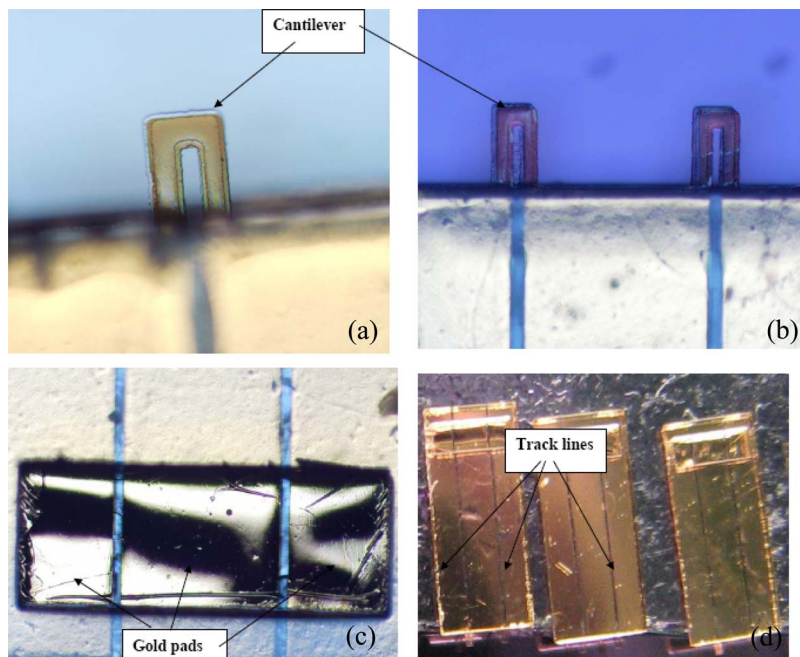


Fig. 4. Optical images of a die with SU-8/polysilicon/SU-8 cantilever. (a) Single cantilever. (b) Cantilevers in half-bridge configuration. (c) Gold pads and track lines. (d) Entire die.

cantilever holder of an AFM, i.e., 1.6 mm wide and 3.4 mm long. The thickness of the die was chosen to be  $300\ \mu\text{m}$  so that the spring of the AFM's cantilever holder could hold it firmly. With these device dimensions, the cantilever die could be fitted in the AFM's cantilever holder, and its resonant frequency could be measured.

The base of the cantilever die was fabricated using SU-8 2100 which is a highly viscous and, therefore, "thick" negative photoresist. The resist was poured on the substrate in such a way that air did not get trapped between the resist layers. This was achieved by spinning the substrate slowly at about 15 r/min while the resist was being poured. To ensure that the resist spreads uniformly on the substrate, it was subsequently spun at 300 r/min for 15 s. The desired final thickness of this layer, i.e.,  $300\ \mu\text{m}$  was achieved by a final spin at 1000 r/min for 1 min. It should, however, be noted that the coated layer thickness substantially depends on the spin cycle [Fig. 3(g) and (m)].

#### H. Release

The die was released from the substrate by etching the sacrificial (sputtered) oxide in hydrofluoric acid [Fig. 3(h)]. When the acid dissolved the oxide completely, the dies simply lifted off from the substrate. An important advantage of this method is that it does not "consume" the substrate as in surface or bulk micromachining. Hence, the substrate is reusable, thereby further lowering the manufacturing cost. Images of the SU-8/polysilicon/SU-8 piezoresistive cantilever captured using an optical microscope are shown in Fig. 4. The close-up view of the cantilever is shown in Fig. 4(a), whereas the entire half-bridge die is shown in Fig. 4(b); the gold pads and tracks are seen in Fig. 4(c), and the entire die is shown in Fig. 4(d).

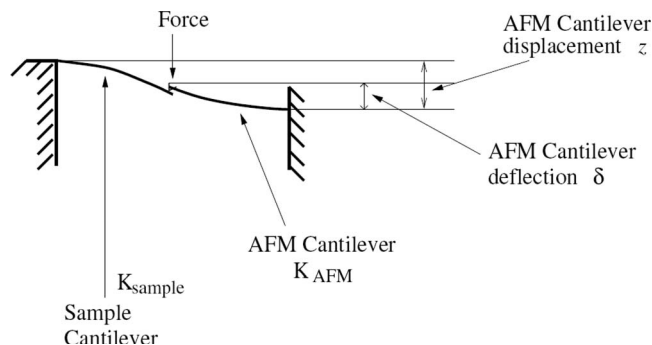


Fig. 5. Schematic for mechanical characterization of cantilever (adopted from [13]).

## IV. DEVICE CHARACTERIZATION

A mechanical characterization of the cantilever was performed to determine its stiffness and the resonant frequency. An electromechanical characterization of the cantilever was performed to quantify the change in resistance of one of the levers for a given deflection at its tip.

### A. Measurement of Stiffness of Cantilever

The mechanical characterization of the cantilever was performed by the technique developed by Serre *et al.* [13]. The technique is based on the measurement of the deflection of the tip of the sample cantilever, due to a load applied on it, by an AFM cantilever, as shown in Fig. 5 (adapted from [13]). The measurement method is briefly explained as follows. The AFM cantilever movement is controlled by a high-precision piezoelectric stage. Its deflection is measured with almost atomic precision by a photodetector. The *approach curve*, which plots the deflection versus displacement of the AFM cantilever, is

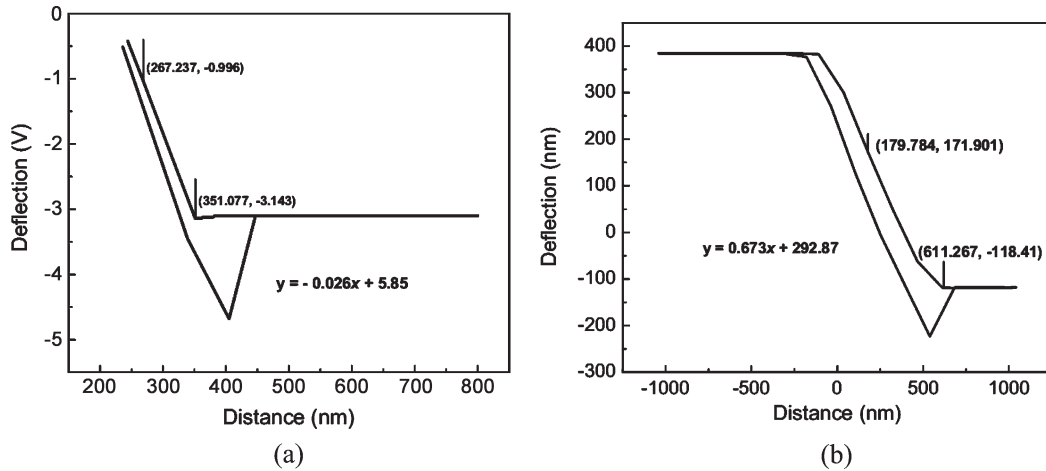


Fig. 6. (a) AFM force versus distance spectroscopy. (b) AFM calibrated force versus distance spectroscopy.

obtained when the probe approaches the sample cantilever and is retracted back from it.

The total displacement of the AFM cantilever is the sum of its own deflection and the bending of the sample cantilever. In the elastic domain, the AFM cantilever bending the sample cantilever forms a system of two springs in series. The overall spring constant of the system is  $K_{total} = (K_{AFM} \cdot K_{sample}) / (K_{AFM} + K_{sample})$ , where  $K_{AFM}$  and  $K_{sample}$  are the spring constants of the AFM and sample cantilevers, respectively. If the two cantilevers are aligned, then the torsional component will be absent, and for a loading force  $F$ , it can be shown that  $K_{total}z = K_{AFM}\delta$  [13], where  $z$  is the deflection of the AFM cantilever and  $\delta$  is the displacement of the sample cantilever. The spring constant of the combined system  $K_{total}$  can be extracted from the slope of the approach curve that is obtained *after* contact of the AFM cantilever is established with the sample cantilever. Finally, the stiffness of the sample cantilever can be calculated as  $K_{sample} = K_{total} \cdot K_{AFM} / (1 - K_{total})$ .

### B. Cantilever Stiffness Measurement Procedure

*Molecular Imaging* AFM was used to measure the stiffness (i.e., its spring constant) of the *SU-8/polysilicon/SU-8* cantilever. The AFM cantilever chosen was a silicon nitride structure whose nominal stiffness was 0.12 N/m (i.e.,  $K_{AFM} = 0.12$  N/m). The stiffness of the AFM cantilever was chosen to be comparable to the stiffness of the *SU-8/polysilicon/SU-8* cantilever as computed by the simulation study (0.31 N/m). This enables the effective spring constant  $K_{total}$  to be about half of the stiffness of either of the cantilevers, thereby allowing maximum response (see expressions for  $K_{total}$ ,  $K_{AFM}$ , and  $K_{sample}$ ).

The AFM cantilever was positioned on the *SU-8/polysilicon/SU-8* cantilever, and it was made to approach the tip of the *SU-8/polysilicon/SU-8* cantilever. To obtain the approach curve, i.e., the “AFM force versus distance spectroscopy,” the deflection versus distance sweep was run. The plot for the approach curve, i.e., “force versus distance spectroscopy,” as the AFM cantilever approaches the *SU-8/*

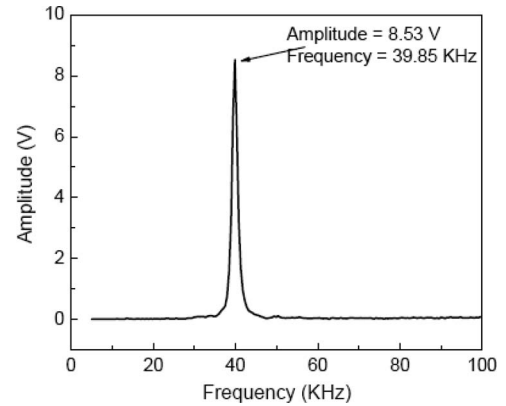


Fig. 7. Frequency response of the *SU-8/polysilicon/SU-8* cantilever.

*polysilicon/SU-8* cantilever is shown in Fig. 6(a). The left and right cursors are placed on the *contact* portion of the curve [Fig. 6(a)]. Thus, one obtains information about the distance traveled by the scanner tube ( $x$ -axis) and the corresponding deflection caused at the tip of the AFM probe (in volts). This information, when used in conjunction with the “calibrate” software tool of the AFM, determines the deflection of the AFM tip in nanometers per volt. The calibration information is also depicted in the text box as  $y = -0.026x + 5.85$ .

Next, the measurement involving the actual bending of the probe cantilever, i.e., “AFM calibrated force versus distance spectroscopy,” was carried out. The deflection of the AFM cantilever in nanometers plotted as a function of the distance traveled by the scanner tube (in nanometers) is shown in Fig. 6(b). These values were used to calculate the value of “ $z$ ” and “ $\delta$ ,” and therefore, the stiffness of the *SU-8/polysilicon/SU-8* cantilever was determined. From this measurement, the following data were extracted. The spring constant of the two-cantilever system was 0.673 (i.e.,  $K_{total} = 0.673$  N/m). This can also be extracted from the position of the cursor marks, i.e., deflection of AFM cantilever  $\div$  distance traveled by  $z$ -piezo, or  $(179.901 - (-118.415)) \div (611.267 - 179.784)$  as observed from Fig. 8. Using the stiffness data of the AFM cantilever ( $K_{AFM} = 0.12$  N/m), the spring constant or stiffness of the *SU-8/polysilicon/SU-8* cantilever was determined from

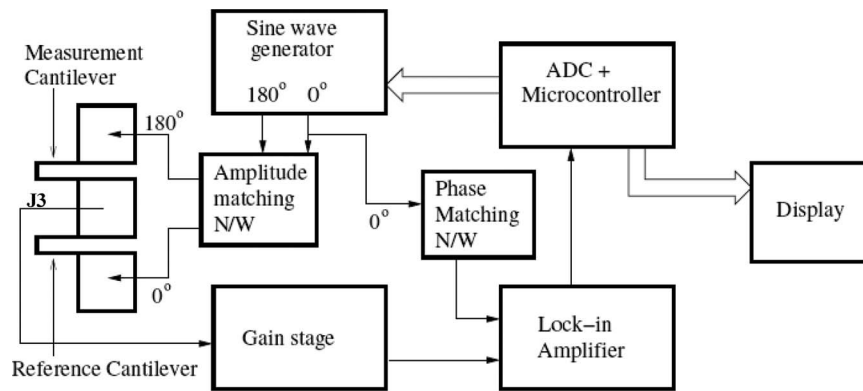


Fig. 8. Functional block diagram of the characterization setup to measure  $\Delta R/R$ .

the equation  $K_{\text{sample}} = K_{\text{total}} \cdot K_{\text{AFM}} / (1 - K_{\text{total}})$  and was computed to be 0.25 N/m.

### C. Measurement of Resonant Frequency of Cantilever

In this measurement, the AFM cantilever was operated in its noncontact or ac mode, and the “frequency response” of the cantilever was obtained. In this mode, the base of the microcantilever die was fitted in the cantilever holder of the AFM, which thereby gets mechanically coupled to the piezoelectric stage. The probing tip therefore gets vibrated by the piezoelectric vibrator. The frequency was swept. The *ac* component of the signal from the photo diode caused by the cantilever vibrations is amplified and directed to the input of the synchronous detector, which forms a signal proportional to the amplitude of vibrations [14]. In the initial attempts to measure the resonant frequency, it was observed that the signal reflected from the cantilever surface was not sufficient. Therefore, there was no way for the feedback electronics to track the vibrating cantilever. To obtain a better reflecting surface on the cantilever, a thin (25 nm) coating of gold was deposited on one surface of the cantilever. The thickness of the gold was kept low enough so as *not* to alter the mechanical properties of the cantilever.

The plot of the signal voltage versus the oscillation frequency of the piezoelectric stage is shown in Fig. 7. The resonant frequency of the fabricated SU-8/polysilicon/SU-8 cantilever was measured to be about 39 kHz. Another parameter of interest is the *Q* of the resonance, which is computed as the ratio of the resonant frequency to the frequency span between the  $-3$ -dB points. *Q* is a measure of the dissipation mechanisms that damp the oscillations of the cantilever. A cantilever with a high *Q* will need a small amount of energy to be excited at its resonant frequency, and its frequency spectrum will consist of a tall narrow peak. On the other hand, a cantilever with a low *Q* oscillates at a lower magnitude for the same energy, and its frequency spectrum is broader [15]. The *Q* value computed for the fabricated cantilever was determined from the equation  $Q = f_0 / (\Delta f_{3\text{ dB}})$  and was calculated to be  $Q = 39\,849\text{ Hz} / (40\,804 - 39\,894\text{ Hz})$  or 43.8. The resonant frequency and *Q* of the device are high enough so that it is not affected by the  $1/f$  noise (up to 50 Hz) and the thermomechanical noise (up to 5 kHz). Therefore, it can find application as a surface-stress sensor.

### D. Electromechanical Characterization

An important performance parameter of a piezoresistive cantilever is its deflection sensitivity. It is a measure of the relative change in resistance as a function of cantilever deflection. The measurement was performed by deflecting the sample cantilever by a micromanipulator. The relative change in resistance was measured using a highly sensitive and in-house-developed electromechanical characterization system. The functional block diagram of the measurement system is shown in Fig. 8.

The measurement system is described as follows. The sine wave generator produces two waveforms of  $0^\circ$  and  $180^\circ$  phases, but of same amplitude and frequency. The  $0^\circ$  waveform is considered as reference signal and fed to the reference cantilever as well as to one of the lock-in amplifier inputs. The  $180^\circ$  phase shifted sine wave is used with the measuring cantilever. The common node from the cantilevers is connected to the other input of the lock-in amplifier through a gain stage. The lock-in amplifier detects the small change in voltage due to the strained cantilever, which is usually buried in noise. It consists of a synchronous detector and a large time constant low-pass filter which collectively helps to achieve such performance. The output dc voltage is converted to digital word through a high-resolution analog-to-digital converter, which is read by the microcontroller, and the result is displayed onto a display screen.

Three micromanipulators of a *Karl Suss PM8* probe station were used to probe the three gold pads, while the fourth micromanipulator of the probe station was used to deflect the cantilever. The advantages of using such a probe station are as follows: 1) the entire die (cantilevers + base, the electrical contact gold pads) can be viewed under its microscope; 2) probing the pads is easy; 3) the tungsten probe (tip diameter  $7\ \mu\text{m}$ ) can be accurately placed on the tip of the cantilever; and 4) the test bench can be firmly held in position on the chuck of the probe station with the aid of a vacuum.

The cantilever piezoresistors were tested for continuity, and their resistance was measured using an electrometer. The nominal value of resistance of one cantilever arm was measured to be 110 k $\Omega$ . Next, in the voltage measurement mode of the electrometer, the voltage was nulled to make the setup ready to measure the change in voltage due to the deflection of one of the cantilevers. The tip of one of the cantilevers (measurement cantilever) was deflected with a micromanipulator probe tip, and

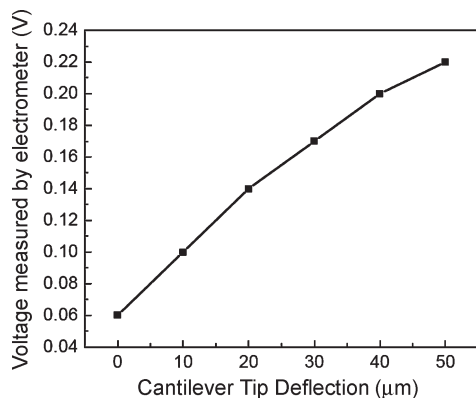


Fig. 9. Change in voltage across the deflected cantilever versus deflection at the tip of the cantilever.

the change in voltage was measured by rotating the micrometer screw by one division (corresponding to a downward movement of the probe tip by 10  $\mu\text{m}$ ). The plot of the measured change in voltage, as the cantilever was deflected, is shown in Fig. 9. We observed that the voltage measured at node J3 (Fig. 8) changed as the cantilever was deflected. This occurred because the deflected cantilever got strained; due to which, its resistance changed, thereby causing a “voltage measure” at the previously nulled node. This clearly established the piezoresistive behavior by the encapsulated polysilicon layer.

To summarize this section, the fabricated polymer cantilever that included an encapsulated polysilicon piezoresistor was successfully characterized. Its stiffness and resonant frequency were determined with the aid of an AFM setup. For its electromechanical characterization, one of the two cantilevers of the die, which formed a balanced (and nulled) half bridge, was deflected, and a change in voltage across it was measured to establish its piezoresistive behavior.

Thus, we demonstrate, for the first time, a photoplastic MEMS device that included an encapsulated polysilicon piezoresistor. The device was designed and fabricated so that it could fit into the cantilever holder of an AFM to enable it to be used in conjunction with an AFM’s liquid cell for biochemical sensing applications. Antibodies, such as antimyoglobin, could be immobilized on one surface of the cantilever inside the AFM’s liquid cell. The scheme could be used to detect myoglobin, a cardiac marker, which is released when a person has a heart attack.

## V. CONCLUSION

In this paper, we have reported, for the first time, the fabrication of a polymeric microcantilever with an encapsulated polysilicon piezoresistor, using a five-mask process. The process to fabricate the die was developed in such a way that it can be lifted off the silicon substrate, making the silicon substrate reusable. The polysilicon piezoresistor was fully encapsulated by SU-8, so that the wet biochemicals do not short the piezoresistors. The devices were characterized for their mechanical and electromechanical behaviors. The spring constant of the fabricated SU-8/polysilicon/SU-8 cantilevers was measured to be 0.25 N/m, while its resonant frequency was ex-

perimentally determined to be about 39 kHz. The piezoresistive properties of these cantilevers, with an encapsulated HWCVD polysilicon piezoresistor, were demonstrated and characterized and were shown to be working well.

## REFERENCES

- [1] R. Raiteri, M. M. Grattarola, H. Butt, and P. Skaldal, “Micromechanical cantilever-based biosensors,” *Sens. Actuators B, Chem.*, vol. 79, no. 2/3, pp. 115–126, Oct. 2001.
- [2] J. Fritz *et al.*, “Translating biomolecular recognition into nanomechanics,” *Science*, vol. 288, no. 5464, pp. 316–318, Apr. 2000.
- [3] J. Thaysen, “Cantilever for biochemical sensing integrated in a micro-liquid handling system,” Ph.D. dissertation, Tech. Univ. Denmark, Copenhagen, Denmark, 2001.
- [4] Y. Arntz *et al.*, “Label-free protein assay based on a nanomechanical cantilever array,” *Nanotechnology*, vol. 14, no. 1, pp. 86–90, Jan. 2003.
- [5] F. Battiston *et al.*, “A chemical sensor based on a microfabricated cantilever array with simultaneous resonance frequency and bending readout,” *Sens. Actuators B, Chem.*, vol. 77, no. 1, pp. 122–131, Jun. 2001.
- [6] R. Berger *et al.*, “Micromechanical thermogravimetry,” *Chem. Phys. Lett.*, vol. 294, no. 4, pp. 363–369, Sep. 1998.
- [7] H. Jensinius *et al.*, “A microcantilever-based alcohol vapor sensor-application and response model,” *Appl. Phys. Lett.*, vol. 76, no. 18, p. 2615, May 2000.
- [8] J. Shaw, J. Gelorme, N. LaBianca, W. Conley, and S. Holmes, “Negative photoresists for optical lithography,” *IBM J. Res. Develop.—Optical Lithography*, vol. 41, no. 1/2, pp. 81–94, Jan.–Mar. 1997.
- [9] S. Mukherji, R. Lal, V. R. Rao, R. O. Dusane, M. Joshi, and N. Kale, “A novel dry method of surface modification of SU8 for immobilisation of biomolecules using hotwire induced pyrolytic process,” *Indian Patent* 213 504, Nov. 25, 2004.
- [10] N. Kale and V. Rao, “Design and fabrication issues in affinity cantilevers for bioMEMS applications,” *J. Microelectromech. Syst.*, vol. 15, no. 6, pp. 1789–1794, Dec. 2006.
- [11] N. Kale, “Making hotwire CVD a viable technology alternative for bioMEMS applications: Device optimization, fabrication and characterization,” Ph.D. dissertation, IIT Bombay, Mumbai, India, 2008.
- [12] C. Savayo *et al.*, “Fabrication and characterization of a micromechanical sensor for differential detection of nanoscale motions,” *J. Microelectromech. Syst.*, vol. 11, no. 6, pp. 703–708, Dec. 2002.
- [13] C. Serre *et al.*, “Measurement of micromechanical properties of polysilicon microstructures with an atomic force microscope,” *Sens. Actuators A, Phys.*, vol. 67, no. 1–3, pp. 215–219, May 1998.
- [14] V. Shashkin, *AFM Characterization of Microlevers*. [Online]. Available: <http://www.nanoworld.org/NanoLibrary/SPM2004/239.pdf>
- [15] J. Tamayo, A. Humphris, A. Malloy, and M. Miles, “Chemical sensors and biosensors in liquid environment based on microcantilevers with amplified quality factor,” *Ultramicroscopy*, vol. 86, no. 1, pp. 167–173, Jan. 2001.



**Nitin S. Kale** received the Ph.D. degree in electrical engineering from the Indian Institute of Technology (IIT) Bombay, Mumbai, India.

After a stint of over a year at TSMC Ltd., he joined the Centre for Nanoelectronics, IIT Bombay, as a Senior Research Associate. His research interests include the design, simulation, fabrication, and characterization of MEMS structures; vacuum system design; and thin films and their characterization from the MEMS perspective.





**Sudip Nag** received the B.E. degree (with highest honors and distinction) from Nagpur University, Nagpur, India, in 2004. He is currently working toward the Ph.D. degree with the Indian Institute of Technology (IIT) Bombay, Mumbai, India, developing a nanoelectronic retinal prosthetic system as a part of his Ph.D. thesis.

After graduation, he joined as a Research Assistant (Fellow) with the Department of Electrical Engineering, IIT Bombay, where he developed the smallest wearable computer for smart monitoring of cardiac patients, named the "Silicon Locket." During 2002-2004, he was a Visiting Student with the Variable Energy Cyclotron Centre, Department of Atomic Energy, Government of India, where he designed and developed a radiation-hardened electronic controller for remote operation of nuclear plants. His research interest includes mixed-signal systems, bioinstrumentation, nanofabrication, and biocharacterization.

Mr. Nag was the IEEE Student Branch Vice Chairman at the undergraduate institute and held several officer positions at the graduate institute. He was a recipient of the Budding Innovators Award 2008, the IEEE ISSS-MDBS 2006 Student Award, the Academic Excellence Award 2004, and the First Prize awards in competitions at various levels.



**Richard Pinto** received the B.Sc. degree from the University of Mysore, Mysore, India, in 1963 and the Ph.D. degree from Tata Institute of Fundamental Research (TIFR), University of Mumbai, Mumbai, India, in 1972, for his work on high-field effects in disordered semiconductors.

In 1964, he joined TIFR as a Member of Research Staff. Here, he set up a fine thin-film laboratory at the erstwhile Solid State Electronics Group and initiated work on disordered (amorphous) semiconductors in the late 1960s. Subsequently, he set up a silicon device processing facility at TIFR and initiated work on charge-coupled imaging devices. After the advent of high-T<sub>c</sub> superconductors in 1986, he established an advanced laboratory at TIFR for the growth of high-T<sub>c</sub> thin films and microwave devices in 1990. He also led a program in this area, which realized the highest critical current density and lowest microwave surface resistance in high-T<sub>c</sub> Ag-doped YBCO thin films. In 2002, he joined the Microelectronics Group, Department of Electrical Engineering, Indian Institute of Technology Bombay, Mumbai, as a member of faculty to work on advanced silicon devices. He has played a key role in setting up an advanced nanoelectronics laboratory at the Centre of Excellence in Nanoelectronics. He has authored nearly 200 research papers published in referred journals. He has organized two international conferences in high-T<sub>c</sub> superconductors and colossal magnetoresistance manganites and has edited two book proceedings. His current interests are in the area of microelectromechanical systems, nanoelectromechanical systems, and nanoelectronics based on silicon and silicon plus materials.



**V. Ramgopal Rao** (M'98-SM'02) received the M.Tech. degree from the Indian Institute of Technology (IIT) Bombay, Mumbai, India, in 1991 and the Dr. Ing. degree from the Universitaet der Bundeswehr Munich, Munich, Germany, in 1997.

From 1997 to 1998 and again in 2001, he was a Visiting Scholar with the Department of Electrical Engineering, University of California, Los Angeles. He is currently a Professor with the Department of Electrical Engineering, IIT Bombay. He is also the Chief Investigator for the Centre for Nanoelectronics, IIT Bombay, besides being the Principal Investigator for many ongoing sponsored projects funded by various multinational industries and government agencies. He is also a member of the working group on nanotechnology set up by the Ministry of Communications and Information Technology, Government of India. His research interests include physics, technology, and characterization of silicon CMOS devices for logic and mixed-signal applications, bio-MEMS, and nanoelectronics. He has authored more than 200 papers published in refereed international journals and conference proceedings in the aforementioned areas. He is the holder of two patents with eight pending.

Dr. Rao is a Fellow of the Indian National Academy of Engineering and the Institution of Electronics and Telecommunication Engineers. He is an Editor of the IEEE TRANSACTIONS ON ELECTRON DEVICES in the CMOS devices and technology area and is a Distinguished Lecturer of the IEEE Electron Devices Society. He was the Organizing Committee Chair for the 17th International Conference on VLSI Design and the 14th International Workshop on the Physics of Semiconductor Devices. He served on the program/organizing committees of various international conferences, including the 2008 International Electron Devices Meeting, the IEEE Asian Solid-State Circuits Conference, the 2006 IEEE Conference on Nano-Networks, the ACM/IEEE International Symposium on Low Power Electronics and Design, and 11th IEEE VLSI Design and Test Symposium. He was the Chairman of the IEEE AP/ED Bombay Chapter from 2002 to 2003 and currently serves on the Executive Committee of the IEEE Bombay Section, besides being the Vice Chair of the IEEE Asia-Pacific Regions/Chapters Subcommittee. He was the recipient of the Shanti Swarup Bhatnagar Prize in Engineering Sciences in 2005 for his work on electron devices; the Swarnajayanti Fellowship Award for 2003-2004, instituted by the Department of Science and Technology, Government of India, the 2007 IBM Faculty Award; and the 2008 "The Materials Research Society of India Superconductivity and Materials Science Prize."